3D Fibrous Tissue Closure and New ECM Deposition is Modulated by ECM Alignment of Adjacent Tissue

Shoshana L. Das[1,2,3], Prasenjit Bose[4], Michael L. Smith[2], Daniel H. Reich[4], Emma Lejeune[5], Christopher Chen[2,3], Jeroen Eyckmans[2,3]

[1]Harvard-MIT Program in Health Sciences and Technology, Institute for Medical Engineering and Science, Massachusetts Institute of Technology,
[2]Department of Biomedical Engineering, Boston University, [3]Wyss Institute for Biologically Inspired Engineering, Harvard University,
[4]Department of Physics and Astronomy, Johns Hopkins University, [5]Department of Mechanical Engineering, Boston University

Introduction

The assembly of provisional matrix is a critical step in wound closure. To close, a wound contracts and fibroblasts move into the gap to lay down a provisional matrix which becomes the template for other cells to migrate upon.

In epithelial cells, the shape of a wound has been shown to correlate with closure rates, i.e. concave gaps close faster compared to convex ones [1]. Shape has also been suggested to control new matrix formation by fibroblasts in models of tissue growth into pores [2].

Fibroblasts rely on interactions with the extracellular matrix (ECM) they are embedded in to mediate migration and contraction. Therefore, we sought to understand how the underlying architecture of their surrounding ECM affects their closure processes, particularly fibroblasts' ability to build provisional matrix to fill a gap.

In this study, we use a tension-based model of 3D stromal gap closure [3] to create microtissues with different ECM alignments and investigate the ability for fibroblasts to assemble provisional matrix to close a gap.

Methods

Device seeding: Microfabricated arrangements of flexible micropillars were seeded with NIH 3T3 fibroblasts embedded in a collagen matrix [3] to create arrays of microtissues with differing ECM alignments [4].

Microtissues with fluorescently-tagged ECM: Human fibronectin (FN) and rat tail collagen I were conjugated to Alexa Fluor 488 and Alexa Fluor 555, respectively. Tagged ECM was added to microtissues during tissue formation, then imaged on confocal or over time on widefield setup with temperature and CO_2 control.

Fiber analysis: A MATLAB code based on Fibriltool [4] measured the alignment angle and average anisotropy of FN of microtissues 10 hours into the healing process.

Figure 1. Fibroblast seeded collagen-based microtissues. a) Anisotropic microtissue 24 hours after seeding, before injury. **b)** Isotropic microtissue 24 hours after seeding, before injury. (Scale bars = 300μm)

Acknowledgements

Funding: NSF (CMMI-1462710, CMMI-1463011) and NIH (EB028491) S.L.D. by NSFGRF (1122374).

References: [1] Vedula, S.R.K., *Nat Comm*, 2015, 6:6111. [2] Bidan, C.M. *Adv Healthcare Mater* 2013, 2:186–194 [3] Sakar, M.S. *Nat Comm* 2016, 7:11036. [4] Bose, P. ACS *Biomater Sci Eng* 2019, 5:3843−3855.

Results

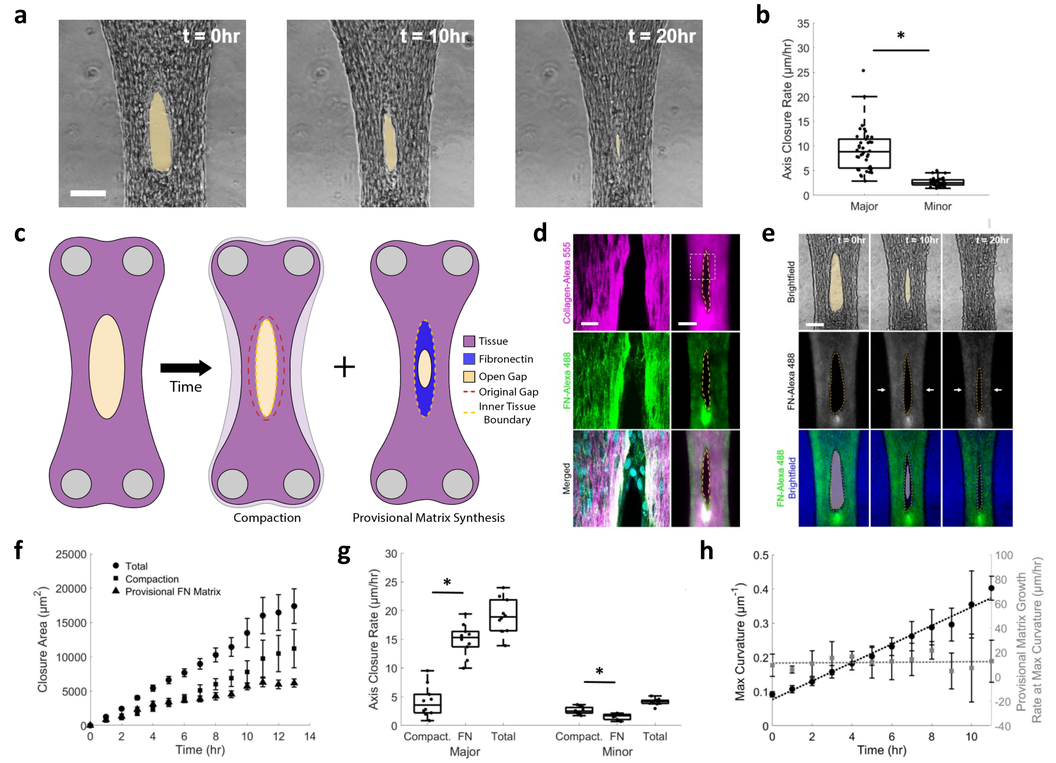

Figure 2. Assembly of fibronectin provisional matrix occurs primarily along the major axis and is not correlated with the curvature of the gap edge. a) Injured anisotropic microtissue spontaneously closing post-injury (Scale bar = 100μm). **b)** Rates (linear) of gap axes closure (n = 38). **c)** Schematic of contributions of both tissue compaction and provisional FN matrix to closure process. **d)** Tissue at 10 hrs post-injury labeled with Collagen-Alexa 555 (magenta), FN-Alexa 488 (green), nuclei (cyan) at 40x confocal (left, scale bar = 25μm) and 10x widefield (right, scale bar = 100μm). Dashed yellow line indicates the inner tissue boundary. **e)** Widefield imaging of tissue with FN-Alexa 488 after injury at t = 0, 10, 20hrs. Brightfield (top), FN-Alexa 488 (middle), and merged (bottom, brightfield (blue), FN-Alexa 488 (green)). Yellow indicates open gap, arrows indicate compaction, dashed yellow line indicates inner tissue boundary. **f)** Total closure (circles) broken down into the contribution of compaction (squares) and FN (triangles) (n = 10). **g)** Major and minor axes linear closure rates broken down into the contribution of compaction and fibronectin (n = 10). **h)** Maximum curvature of gap over time (left axis, circles) and provisional matrix growth rate at point of maximum curvature over time (right axis, squares).

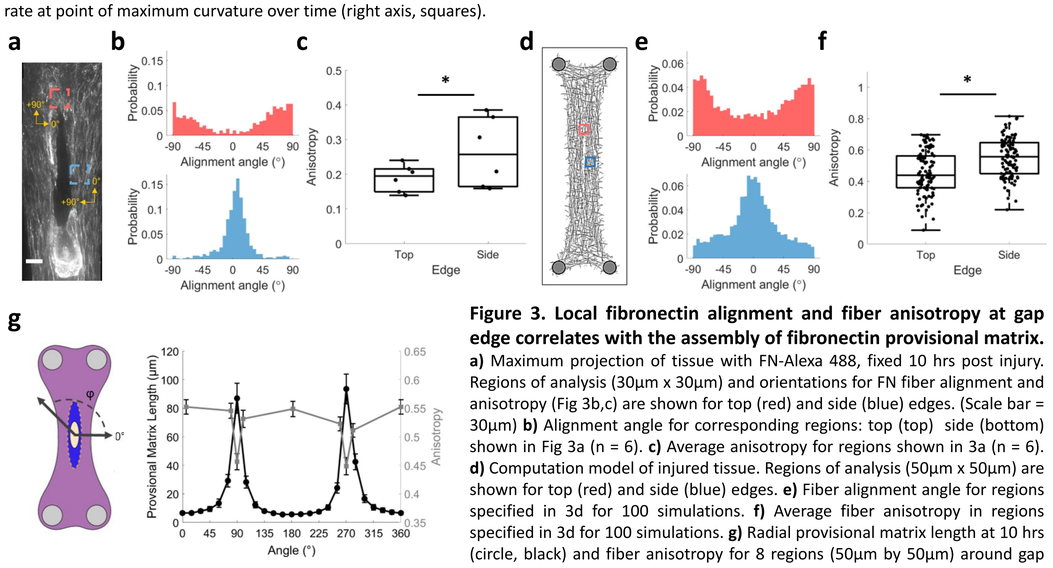

Figure 3. Local fibronectin alignment and fiber anisotropy at gap edge correlates with the assembly of fibronectin provisional matrix. **a)** Maximum projection of tissue with FN-Alexa 488, fixed 10 hrs post injury. Regions of analysis (30μm x 30μm) and orientations for FN fiber alignment and anisotropy (Fig 3b,c) are shown for top (red) and side (blue) edges. (Scale bar = 30μm) **b)** Alignment angle for corresponding regions: top (top) side (bottom) shown in Fig 3a (n = 6). **c)** Average anisotropy for regions shown in 3a (n = 6). **d)** Computation model of injured tissue. Regions of analysis (50μm x 50μm) are shown for top (red) and side (blue) edges. **e)** Fiber alignment angle for regions specified in 3d for 100 simulations. **f)** Average fiber anisotropy in regions specified in 3d for 100 simulations. **g)** Radial provisional matrix length at 10 hrs (circle, black) and fiber anisotropy for 8 regions (50μm by 50μm) around gap from model (square, gray).

Results

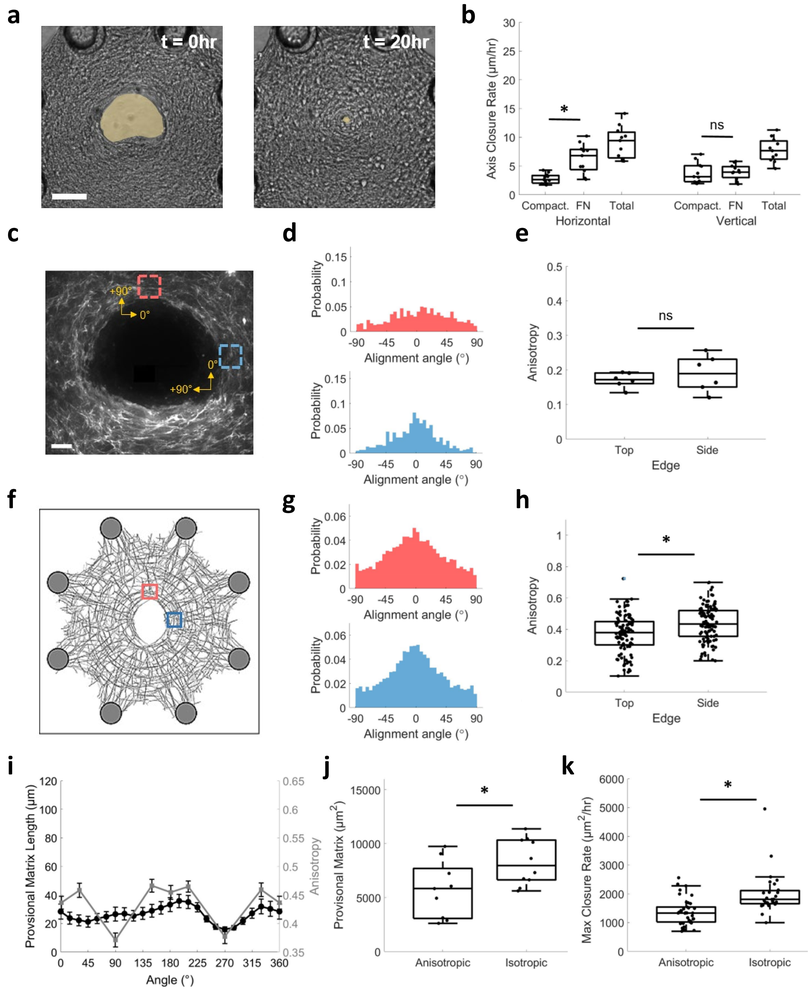

Figure 4. Isotropic tissue has more uniform, but less ECM alignment, and heals faster with more provisional matrix deposition. a) Injured isotropic microtissue spontaneously closing post-injury (Scale bar = 100μm) **b)** Horizontal and vertical axes linear closure rates broken down into the contribution of compaction and fibronectin (n = 10 tissues). **c)** Maximum projection of tissue with FN-Alexa 488, fixed 10 hrs post injury. Regions of analysis (30μm x 30μm) and orientations for FN fiber alignment and anisotropy (Fig 4g,h) are shown for top (red) and side (blue) edges. (Scale bar = 30μm) **d)** Alignment angle for corresponding regions: top (top) side (bottom) shown in Fig 4c (n = 6). **e)** Average anisotropy for regions shown in 4c (n = 6). **f)** Computation model of injured tissue. Regions of analysis (50μm x 50μm) are shown for top (red) and side (blue) edges. **g)** Fiber alignment angle for regions specified in 4f for 100 simulations. **h)** Average fiber anisotropy in regions specified in 4f for 100 simulations. **i)** Radial provisional matrix length at 10 hrs (circle, black) and fiber anisotropy for 8 regions (50μm by 50μm) around gap from model (square, gray). **j)** Total provisional matrix at 10hrs for isotropic and anisotropic tissues. **k)** Maximum closure rates for isotropic and anisotropic tissues.

Conclusion

Our study suggests that the ability for fibroblasts to build provisional matrix into a gap is affected by the structure of surrounding ECM. Regions with higher FN fiber alignment and anisotropy have less provisional matrix deposition. Furthermore, less-aligned isotropic tissues have more overall provisional matrix assembly and faster closure rates. This suggests ECM alignment may act as a negative regulator of matrix assembly within wounds.